ISBN: 978-3-95450-201-1 doi:10.18429/JACoW-IBIC2018-WEPA19

# RESULTS FROM THE CERN LINAC4 LONGITUDINAL BUNCH SHAPE MONITOR

J. Tan†, G. Bellodi, CERN, Geneva, Switzerland
A. Feschenko, S. Gavrilov, Institute for Nuclear Research, Moscow, Russia

*Abstract*

The CERN Linac4 has been successfully commissioned to its nominal energy and will provide 160 MeV H⁻ ions for charge-exchange injection into the Proton Synchrotron Booster (PSB) from 2020. A complete set of beam diagnostic devices has been installed along the accelerating structures and the transfer line for safe and efficient operation. This includes two longitudinal Bunch Shape Monitors (BSM) developed by the Institute for Nuclear Research (INR, Moscow). Setting-up the RF cavities of Linac4 involves beam loading observations, time-of-flight measurements and reconstruction of the longitudinal emittance from phase profile measurements. In this paper the BSM is presented along with some results obtained during accelerator commissioning, including a comparison with phase measurements performed using the Beam Position Monitor (BPM) system.

## INTRODUCTION

The Linac4 [1] is an 80 m-long, normal-conducting, pulsed, linear accelerator, providing a 160 MeV H⁻ ion beam every 1.2 s. A block diagram of the machine is shown in Figure 1. It will replace the ageing 50 MeV proton Linac2 as the injector of the PSB in 2020. The motivation for this upgrade is twofold: firstly to overcome the present space charge limitation at PSB injection, doubling the intensity within the same transverse emittance; secondly to minimise beam loss at PSB injection. The latter requirement is achieved with a charge exchange injection, an adequate chopping scheme and longitudinal phase space painting for high intensity beams.

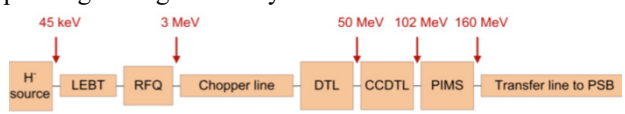


Figure 1: Linac4 schematic layout.

The beam instrumentation specifications [2, 3] along the accelerator and its transfer line must cover the challenging operational parameters summarized in Table 1.

Table 1: Linac4 Parameters and Achievements To Date

| Parameters | Design target | Achieved |
|---|---|---|
| Peak current in the linac | 40 mA | 24 mA |
| Routine current in the linac | 40 mA | 20 mA |
| Transv. Emittance at 160 MeV | 0.4 π.mm.mrad | 0.3π.mm.mrad |
| Energy at PSB injection | 160 MeV | 160 MeV |
| Pulse length / rep. rate | 400 μs / 1 Hz | up to 600 μs/1Hz |

† jocelyn.tan@cern.ch

The achieved performance during the Linac4 commissioning stages from 45 keV to 160 MeV are presented in [4, 5, 6, 7]. Here we present results of longitudinal beam profile measurements performed with the BSMs located in the transfer line, including a comparison with phase measurements performed using the BPM system.

## BEAM PHASE PROFILE DIAGNOSTICS

### *Bunch Shape Monitor*

The BSM principle of operation is explained with Figure 2 and is described in detail elsewhere (see for example [8]). In brief, its operation is based on transforming the longitudinal structure of the beam under study into a transverse distribution of low energy secondary electrons.

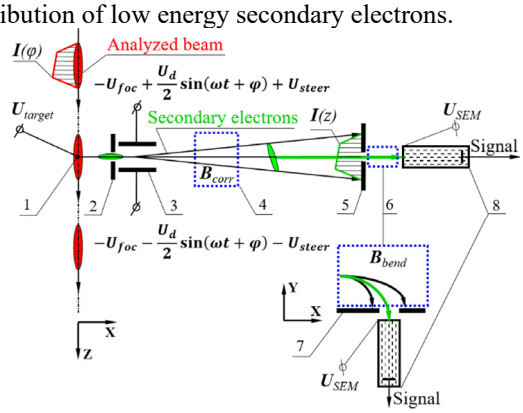


Figure 2: BSM principle: 1-wire target, 2-input collimator, 3- rf deflector combined with electrostatic lens, 4-corrector magnet, 5 and 7- collimators, 6-bending magnet, 8-electron multiplier.

This is achieved by placing a wire target in the beam, which emits secondary electrons in proportion to the instantaneous H⁻ intensity. These electrons are accelerated with a HV applied to the target and converted to a transverse distribution using an RF deflection, from which a specific slice is selected for detection using a collimator. The RF deflector operates at the accelerator frequency $f_{RF}$ of 352.2 MHz. For a fixed setting of the RF deflecting phase with respect to the accelerator reference, the intensity of the secondary electrons passing the collimator and detected with the electron multiplier corresponds to the H⁻ intensity at a specific point of the longitudinal charge distribution of the beam under study. The whole distribution is obtained by scanning the phase of the RF deflecting field through a complete half period. The bending magnet is tuned to select only electrons with an energy corresponding to acceleration from the target potential, and is used to remove any influence from electrons detached from H⁻ ions

ISBN: 978-3-95450-201-1 doi:10.18429/JACoW-IBIC2018-WEPA19



in the target. For each profile, the phase range of the measurements is 180°, with a resolution close to 1°. The phase scan provides one longitudinal point per beam pulse. Nevertheless, the BSM signal is sampled every µs thus providing the longitudinal distribution within the beam pulse. As the complete measurement is performed over many beam pulses, the reproducibility of beam parameters from pulse to pulse is assumed.

Two monitors are currently installed in the transfer line at the end of Linac4, their distance with respect to the last PIMS (π Mode Structure) cavity being respectively 5.55 m and 35 m. When the Linac4 is connected to the PSB in 2020, the final position of the 2nd monitor will be at 63.5 m.

### *Beam Position Monitor*

The beam trajectory measurement system was designed to provide the absolute beam position, the relative beam intensity and the mean beam energy via time-of-flight (TOF) measurements between BPMs. It consists of a set of 42 BPMs, with 15 units installed between the Linac4 RF modules and 27 units spread along the 177 m-long transfer lines to the PSB. Compactness, good linearity and sensitivity to the bunching frequency were the main criteria for selecting shorted striplines pick-ups as the basic sensor [9].

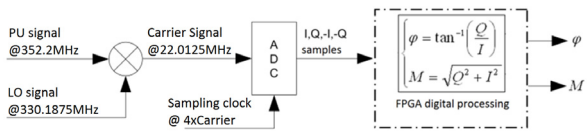


Figure 3: I/Q schematic with $f_{LO} = f_{RF} \cdot 15/16$.

The "I/Q method" [10] as represented in Figure 3, is applied for signal processing. The analog signal from the BPM is filtered to obtain the first RF harmonic which then undergoes down-mixing with a Local Oscillator (LO). The resulting intermediate frequency (IF) is sampled at four times the IF so as to acquire data $\pi/2$ apart. Averaging of I and Q samples over one IF period is performed for noise filtering. From standard trigonometric functions, one then obtains the magnitude M and the relative beam phase for each electrode, as a function of time with a granularity of $1/f_{IF} = 45$ *ns*. The position is computed from the difference in magnitude between two facing electrodes and normalisation with their sum, while the beam intensity is proportional to the magnitude sum of all electrodes.

The strong variation of the BPM sensitivity with bunch velocity (due to the changing energy) along the linac is taken into account during the processing. Table 2 lists the specifications and the present performance.

Table 2: BPM Specifications vs. Achieved Performance

| Parameters | Specifications | Achieved |
|---|---|---|
| Position resolution [mm] | 0.1 | 0.006 |
| Position accuracy [mm] | 0.4 | 0.1 |
| Phase [°] | 0.5 | 0.1 |
| Intensity [mA] | 0.5 | 0.1 |

## MEASUREMENTS

In addition to the determination of longitudinal emittance for optimum RF module settings [11], the BSM has been extensively used to assess qualitatively or quantitatively the longitudinal distribution over the working range of the cavity, as well as for different chopping frequencies. A first comparison with BPMs phase is included.

### *Momentum Spread Measurement for Nominal Settings at 160 MeV*

Figure 4 shows the results of bunch shape measurements with the two BSMs obtained for nominal accelerator settings. The longitudinal phase distribution of the pulse is obtained by integrating all phase profiles over time. In order to minimize errors in the rms size estimate, a 2% cut off level is set as represented by the red lines in Figure 4.

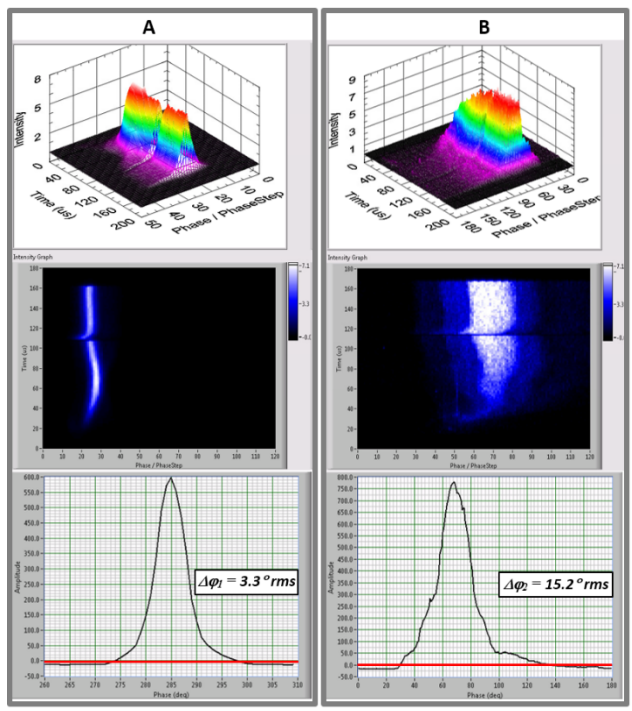


Figure 4: Evolution of the longitudinal bunch profile within the beam pulse observed with the first BSM (A) at the exit of the linac and the second BSM (B) in the transfer line. The phase unit is in degree at 352.2 MHz.

The rms bunch lengths at the first and the second BSMs are $\sigma_1 = 26$ *ps* and $\sigma_2 = 120$ *ps* respectively. The measurements were performed for a low beam current of 5.6 mA. In this case a momentum spread in the beam can be estimated using simple considerations. Two particles with a momentum difference of $\Delta p/p$ after drifting a distance $L$ will be separated longitudinally by the phase interval in degree:

$$\Delta\varphi = \frac{360L}{\lambda\beta\gamma^2} \cdot {}^{\Delta p}/_{p}$$

Here $\beta$ and $\gamma$ are relativistic factors, and $\lambda$ is the RF wavelength. Substituting $\Delta\varphi_2 = 15.2°$ measured by the 2nd BSM, one can estimate the rms ${}^{\Delta p}/_{p} = 7.3 \times 10^{-4}$.

ISBN: 978-3-95450-201-1 doi:10.18429/JACoW-IBIC2018-WEPA19

The simulations performed for a beam current of 62.5 mA [12], show much faster growth of the rms bunch length from 18 ps at the BSM#1 to 140 ps at BSM#2 location and give smaller momentum spread of $6.7\times10^{-4}$ at BSM#2. The larger experimentally estimated momentum spread above is consistent with the wider initial bunch length found at the Linac4 exit.

### *Variation of Chopping Pattern*

Figure 5 shows the evolution of the bunch shape within the beam pulse for three chopping patterns, for a 140 µs-long pulse with optimum cavity settings. The measurement conditions are summarised in Table 3.

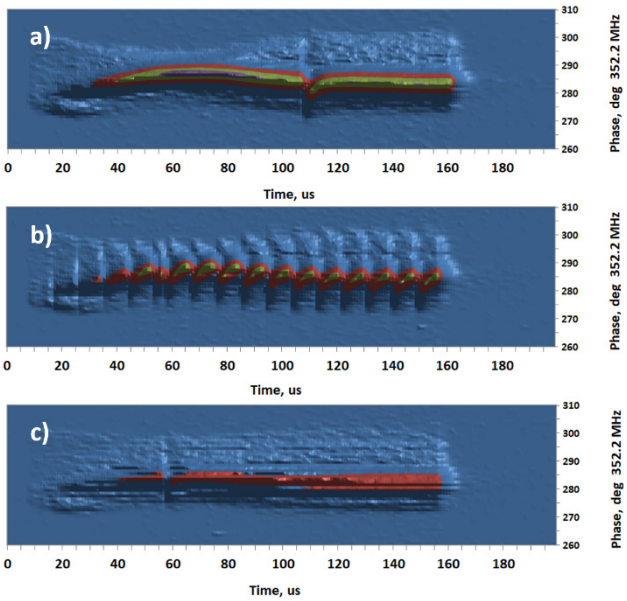


Figure 5: Bunch shape behaviour within the beam pulse for three chopping patterns.

Table 3: Chopper Settings and Rms Bunch Lengths σ

| Parameters | Fig. 5a) | Fig. 5b) | Fig. 5c) |
|---|---|---|---|
| Av. Current [mA] | 17 | 15 | 11 |
| Chopper ON [µs] | 0 | 1 | 0.325 |
| Chopper OFF [µs] | 100 | 8 | 0.625 |
| Duty cycle [%] | 100 | 89 | 62.5 |
| $\sigma$ from BSM [ps] | 26 | 28.4 | 27.6 |

Fig 5a) shows the pulse structure acquired with the chopper off, while in Fig 5b) the chopped beam structure is clearly visible. The plot in Fig 5c) corresponds to a chopping frequency of 1.05 MHz, very close to the nominal LHC chopping pattern at 0.99 MHz. The BMS specification for a low noise acquisition imposes a relatively low amplifier bandwidth of a few hundred kHz after the electron multiplier which, when combined with the BMS signal sampling at 1 MHz means that one cannot detect the chopping frequency. Nevertheless, the effect of the chopping pattern is small, as can be seen from Table 3 where the rms bunch length is only slightly increased when measuring a chopped beam.

### *Phase and Power Scan of PIMS11-12 Cavities*

During the commissioning steps of the linac and later for machine operation, the essential technique for emittance reconstruction is based on analytic calculations with transfer matrices and beam profile measurements. This working principle is valid and applied for both transverse and longitudinal planes [11]. In the latter case, phase or amplitude of an RF cavity is varied to modify the beam phase spread which is measured by a BSM dowstream. With at least three measurements, a matrix inversion calculation gives the initial longitudinal Twiss parametres at the cavity input. Furthermore, a phase shift of a longitudinal profile can be interpreted by a change of transit time, or an energy gain $\Delta E$ given by [13]

$$\Delta E = \frac{\Delta P}{I}$$

with $\Delta P$ as the difference in RF power, and $I$ as the beam current at a dowstream current monitor. This simple and precise method is applied to determine the energy gain through a cavity by beam loading measurement.

The PIMS structure consists of 12 modules powered in pairs. Phase measurements of the PIMS11-12 modules were performed for a beam current of 14 mA with a 200 µs beam pulse duration. A nominal accelerating voltage of 4.1 MV was used. The dependence of the average bunch position (phase with respect to the main RF clock), as measured by the BSM, on the phase of the accelerating field in PIMS11-12 is shown in Figure 6. The phase spread of the measured function is 290.6 ° which in time domain corresponds to a swing of 2.29 ns in the beam transit time between the cavity and the BSM.

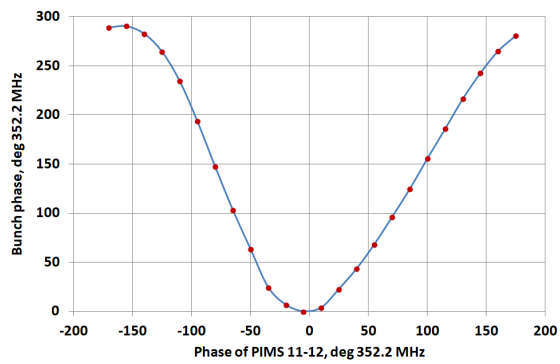


Figure 6: Dependence of average bunch position on the phase of the field in PIMS11-12. The phase spread of the measured function is 290.6 ° (vertical axis). This is equivalent to 2.29 ns of beam transit time swing.

Bunch lengths have been measured for various amplitudes of PIMS11-12 voltage with nominal settings of PIMS1-10. The initial accelerating voltage of PIMS11-12 was the nominal 4.1 MV. The integrated longitudinal profile over the entire beam pulse measured for several RF power levels are presented in Figure 7. Athough the results show a slightly higher profile at 3.1 MV, the rms bunch length here is 6% larger than the nominal one, rising up to

ISBN: 978-3-95450-201-1 doi:10.18429/JACoW-IBIC2018-WEPA19



12% at 0.3 MV. As for the phase scan, the beam transit time swing induced by the power scan is 1.03 ns.

Besides the longitudinal emittance reconstruction, the BSM profiles obtained by phase and power scans can be used to set both the amplitude and phase of the accelerating field by comparing with theoretical functions. For a better understanding of the accelerator it should be interesting to associate RF settings from the BSM with those from BPMs via TOF [14].

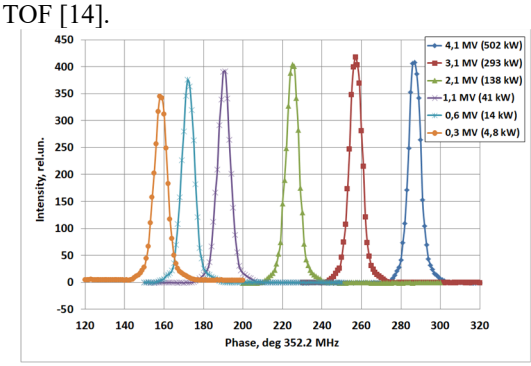


Figure 7: Integrated longitudinal distributions for different accelerating voltages in PIMS11-12. The phase spread (on the horizontal axis) of the peak distribution is 128.5 °. This is equivalent to 1.03 ns of beam transit time swing.

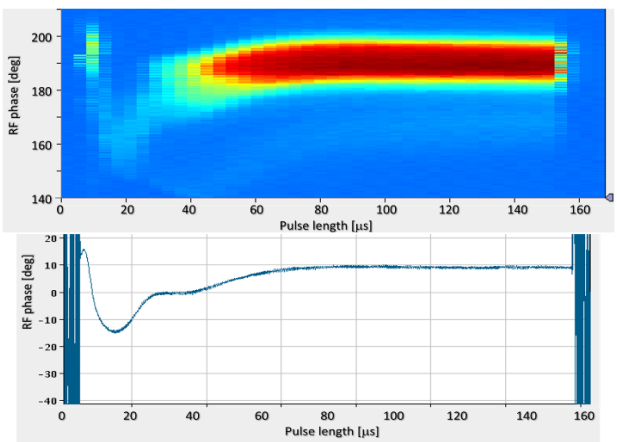


Figure 8: Beam phases in the Linac4 transfer line. Top plot was acquired with the BMS#1. Bottom plot was taken with a nearby BPM.

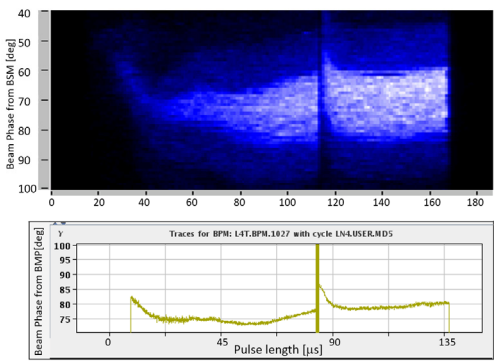


Figure 9: Beam phases in the Linac4 transfer line under different machine settings. Top plot was acquired with the BMS#2. Bottom plot was taken with a nearby BPM.

### *Beam Phase Comparison with the BPMs*

Longitudinal bunch position measurements taken by the BSM were compared to those from a beam position monitor pick-up located ~1 m away. Figure 8 shows the acquisition of a 150 µs-long pulse with BSM#1 and its neighbouring BPM. Figure 9 shows similar plots taken by BSM#2 and a neighbouring BPM upstream under different machine settings, where the pulse was shortened to 130 µs. For each case, one observes a good agreement for the time evolution of the beam phase.

Since the phase information from the stripline pick-ups relies on the function $tan^{-1}$ (see Figure 3), only the non-integer part (modulo $\pi$) of the total phase is known. Furthermore the argument $Q/I$ does not contain information on the particle distribution of the $H^-$ bunches. The phase distribution measured in a single shot by a pick-up is equivalent to the peak distribution of the longitudinal bunch length measured by the BSM, which requires a fine phase scan taking about 50 shots. The BSM is therefore used for phase spread measurements and longitudinal emittance reconstruction, while the BPM phase curve can quickly spot shortcomings in, for example, the cavity beam loading feedback system.

## CONCLUSION

The Bunch Shape Monitor has been extensively used for all the commissioning stages of the Linac4 from 3 MeV to 160 MeV, and to explore and optimise the final settings of the machine. This instrument is complementary to the Beam Position Monitors that are able to give the average time structure of the beam phase in a single shot. Both monitors will be useful after the connection of the Linac4 to the PSB, to validate the new transfer line optics at 160 MeV, for setting up the longitudinal painting scheme for high intensity users, and for optimisation during routine operation.

## ACKNOWLEDGEMENTS

The authors would like to thank J.B. Lallement, A. Lombardi and the BE-OP team for their strong support. U. Raich who was in charge of the BSMs is warmly acknowledged for his genuine contribution. Finally, our special thanks to the INR team, namely Y. Kiselev, V. Gaydash and Y. Gotovtsev for their fruitful collaboration and help in the commissioning of the BSM.

## REFERENCES

[1] F. Gerigk, M. Vretenar (eds.), “Linac4 technical design report”, CERN-AB-2006-084, Dec. 2006

[2] K. Hanke and A. Lombardi, “Beam measurements for Linac4 and its transfer lines”, CERN L4-B-ES-0002, Nov. 2010

[3] F. Roncarolo *et al.*, “Overview of the CERN Linac4 beam instrumentation”, in *Proc. LINAC 2010*, Tsukuba, Japan, Sep. 2010, paper THP007, pp. 770-772.

[4] F. Zocca *et al.*, “Beam diagnostics measurements at 3 MeV of the Linac4 H- beam at CERN”, in *Proc. IPAC 2014*, Dresden, Germany, June 2014, pp. 3694-3696,

ISBN: 978-3-95450-201-1 doi:10.18429/JACoW-IBIC2018-WEPA19

doi.org/10.18429/JACoW-IPAC2014-THPME179

[5] A. Lombardi, "Commissioning of the low-energy part of Linac4", in *Proc. LINAC 2014*, Geneva, Swizerland, Aug.-Sep. 2014, paper MOIOA02, pp.6-10.

[6] U. Raich *et al.*, "Beam instrumentation performance during commissioning of CERN's Linac4 to 50 MeV and 100 MeV", in *Proc. IPAC 2016*, Busan, Korea, May 2016, pp. 293-295, doi.org/10.18429/JACoW-IPAC2016-MOPMR026

[7] F. Roncarolo *et al.*, "Beam Instrumentation for the CERN Linac4 and PSB Half Sector Test", in *Proc. IPAC 2017*, Copenhagen, Denmark, May 2017, pp. 408-411, doi.org/10.18429/JACoW-IPAC2017-MOPAB120

[8] A. Feschenko, "Technique and instrumentation for bunch shape measurements", in *Proc. RUPAC 2012*, Saint-Petersburg, Russia, September 2012, paper FRXOR01, pp.181-185.

[9] J. Tan, M. Ludwig, L. Søby, M. Sordet and M. Wendt, "Commissioning of the CERN Linac4 BPM system with 50 MeV proton beams", in *Proc. IPAC 2013*, Shanghai, China, June 2013, paper MOPWA037, pp. 750-752.

[10] T. Schilcher, "RF applications in digital processing", in *Proc. of CERN Acc. School*, CERN-2008-003, Sigtuna, Sweden, May-June 2007, pp. 249-283.

[11] V. A. Dimov, J.B. Lallement, A. M. Lombardi and R. Gaur, "Emittance reconstruction techniques in presence of space charge applied during the Linac4 beam commissioning", in *Proc. HB2016*, Malmö, Sweden, July 2016, paper WEPM1Y01, pp. 433-438.

[12] L. Hein and A. Lombardi, "Update of the Linac4-PSB Transfer Line", CERN sLHC-Project-Note-0028, Dec. 2010.

[13] A. Lombardi, "The Linac4 project", in *Proc. HB2016*, Malmö, Sweden, July 2016, paper MOAM2P20, pp. 1-5.

[14] M. Bozzolan and J.B. Lallement, "BPM time of flight measurements for setting-up the RF cavities of the CERN Linac4", to be published in *Proc. LINAC 2018*, Beijing, China, Sep. 2018